

ANALYTICAL EVALUATION OF AN ADVANCED INTEGRATED SAFETY SEAT DESIGN IN FRONTAL, REAR, SIDE, AND ROLLOVER CRASHES

Mostafa Rashidy, Balachandra Deshpande, Gunasekar T.J., Russel Morris

EASi Engineering

Robert A. Munson, Jeffrey A. Lindberg

Johnson Controls, Inc.

Lori Summers

National Highway Traffic Safety Administration

United States of America

Paper No. 305

ABSTRACT

Analytical computer simulations were used to optimize and fabricate an Advanced Integrated Safety Seat (AISS) for frontal, rear, side, and rollover crash protection. The AISS restraint features included: dual linear recliners, pyrotechnic lap belt pretensioner, 4 kN load-limiter, extended head restraint system, rear impact energy absorber, seat-integrated belt system, and side impact air bag system. The evaluation and optimization of the AISS design was achieved through analytical simulations using MADYMO multi-body analysis software, LS-DYNA3D finite element software, and through LS-DYNA3D/MADYMO coupling. Frontal and rear impact sled tests were also conducted with physical AISS prototypes and baseline integrated seats to verify performance.

Both the analytical modeling and the experimental sled testing demonstrated safety improvements over the baseline integrated seat. The AISS pyrotechnic lap belt pretensioner and 4 kN load-limiter contributed to a 26 percent reduction in occupant chest acceleration in the frontal impact mode. In the rear impact mode, the AISS dual linear recliners, rear impact energy absorber and extended head restraint system contributed to reducing the occupant upper neck injury parameters. Full vehicle finite element models were used in both the side impact and rollover simulations to evaluate occupant restraint performance. Two generic AISS restraint features were modeled for side impact protection: an inflatable tubular cushion air bag system and a combination head/thorax side impact air bag system. The combination head/thorax side impact air bag system model was found to provide improved occupant protection due to its ability to cover both head and thorax regions and provided a softer reaction surface for the occupant. Upper and lower rib Thoracic Trauma Index (TTI) were reduced 22.1 percent and 14.8 percent, respectively in the side impact simulations. The AISS extended head restraint, pyrotechnic lap belt pretensioner, and seat-integrated belt system also provided benefit in restraining the occupant and minimizing roof crush in the rollover simulations.

INTRODUCTION

U.S national statistics for 1998 reveal that 25,210 drivers were killed and 2,061,000 were injured in motor vehicle crashes [1]. Next to the driver, the right front passenger position accounts for the second most common location of fatalities and injuries among car occupants. Therefore, considerable work has been directed toward improving the protection provided in these two most frequently occupied seating positions.

The initial goal of the Advanced Integrated Safety Seat (AISS) project was to explore the potential for advanced seating system designs to extend occupant protection to all major car crash modes (frontal, rear, side and rollover) [2]. Through a contract from the National Highway Traffic Safety Administration (NHTSA), EASi Engineering, in conjunction with Johnson Controls, Inc., conceived and designed an advanced integrated structural seat that met the current U.S. Federal Motor Vehicle Safety Standard (FMVSS) requirements and improved occupant protection for frontal, rear, side, and rollover crashes and contributed to passenger compartment intrusion resistance.

By focusing on the seat structure modifications, it was thought that the resulting design would be simple and cost efficient. Previous studies have shown that it is possible to develop an integrated structural seat to provide the improved occupant protection and comfort of an integrated seat belt system without the associated cost and weight increases of more complex systems [3]. Therefore, an integrated structural seat was chosen as the baseline seat in the program. Integrated seats have the belt anchorages on the seat itself as opposed to conventional seats where the shoulder belt upper anchorage is located on the car upper body structure. Therefore, the belt fit is considerably improved regardless of the seating position, and the assembly of the seat in the car becomes much easier with this design as the belts are part of the seat. The AISS seat system is also designed to function with the body structure to resist passenger compartment intrusion in side and rollover crashes.

This paper reports on the results of analytical modeling conducted in the frontal, rear, side, and

rollover crash modes, and frontal and rear impact sled tests conducted with AISS prototypes.

RESULTS AND DISCUSSION

Frontal Impact

In the U.S., frontal crashes are the most significant cause of motor vehicle fatalities [4]. Research has found that lap/shoulder belts, when used properly, reduce the risk of fatal injury to front seat passenger car occupants by 45 percent and the risk of moderate-to-critical injury by 50 percent [4]. For light truck occupants, seat belts reduce the risk of fatal injury by 60 percent and moderate-to-critical injury by 65 percent [4]. NHTSA also estimates that drivers protected by air bags experience a reduced fatality risk of 19 percent in all frontal crashes [5]. However, even after full implementation of driver and passenger air bags by FMVSS No. 208, it has also been estimated that frontal impacts will still account for over 8,500 fatalities and 120,000 moderate-to-critical injuries each year [6]. Therefore, the AISS project explored potential seat enhancements that could improve occupant protection beyond the current FMVSS.

AISS Features for Frontal Impact: The AISS design has the following countermeasures for improved occupant crash protection in frontal impacts: pyrotechnic lap belt pretensioner, 4 kN load limiter, integrated seat belt system, and extended head restraint system.

In a frontal impact crash, the pyrotechnic lap belt pretensioner takes up slack in the seat belt and induces energy absorption during the early forward travel of the occupant. When the device is fired, the pretensioner pulls down on a cable that is attached to the belt buckle. This effectively removes the extra slack, and cinches the occupant to the seat. Some studies have reported that this also prevents submarining by narrowing the opening for the pelvis to slide through [7].

A 4kN load limiter was included in the AISS design to reduce the belt loads on the chest while maintaining enough restraint to keep the occupant within the compartment during side and rollover crashes. The upper anchorage of the torso belt on the seat back structure of current integrated seats is the greatest source of seat back bending moment and shear load on the seat structure. By limiting the torso belt loads on the integrated seat, it allows a weight reduction of the seat back structure and reduced floor pan shear while also reducing occupant injuries in frontal crashes. The load limiting retractor of the AISS is designed to let the belt spool out of the retractor at a prescribed load of 4 kN. The 4 kN load limiting designation was based on biomechanical analyses conducted by Kallieris, et

al. [8]. In the AISS design, the retractor is fitted with a torsion bar to provide the load limiting feature.

Analytical Modeling: A coupled LS-DYNA3D/MADYMO model of the AISS was developed and used for design optimization and countermeasure evaluation. The AISS model consisted of the following major structural assemblies: seat pan, seat track, retractor housing, seat belt, recliner, and energy absorber. Figure 1 provides four illustrations of the analytical AISS model. Details of the model have been reported in [3, 9, 10].



Figure 1: Analytical model of the Advanced Integrated Safety Seat (AISS).

For the frontal impact simulation, the MADYMO Hybrid III 50th percentile male dummy model was coupled with the AISS model. The seat belt was modeled and fitted around the dummy using EASi-CRASH software and the belt was anchored at the appropriate locations. The slip ring feature in MADYMO was used to simulate the seat belt sliding at the buckle location. The seat cushion, seat back foam, and knee bolster were modeled as solid elements. The floor pan and toe board assemblies were modeled as shell elements. The finite element geometry of the seat model was based on IGES data provided by Johnson Controls, Inc.

The material and section properties were also supplied by Johnson Controls, Inc. [9]. The welded structural components of the AISS were modeled using nodal rigid bodies. Bar elements were used to simulate the bolts/pins between components. Sliding contact

surfaces were defined between other finite element parts. Geometric contact entities were used to simulate the contact interaction between the seat structure and the dummy. A 0.5 coefficient of friction was applied. The seat back frame, the dual linear recliners, and the rear impact energy absorbers were optimized for frontal and rearward loading. For frontal impact, the seat back was designed not to buckle at a force level of 4 kN, plus an additional 10% percent [9].

The AISS analytical model with a belted MADYMO Hybrid III 50th percentile male dummy was subjected to a frontal impact sled test simulation equivalent to a 56 kmph rigid barrier crash test. A baseline integrated seat model (without advanced features) was also developed and subjected to the identical frontal impact sled test simulation for comparison.

Results of the Analytical Simulations: The AISS frontal impact simulation results were compared to those from the baseline seat (Figure 2). The injury measures were normalized according to the 50th percentile male Hybrid III Injury Criteria Performance Levels (ICPLs) that were proposed in the Notice of Proposed Rulemaking (NPRM) for Federal Motor Vehicle Safety Standard (FMVSS) No. 208 [11]. The referenced ICPLs are listed in Table 1.

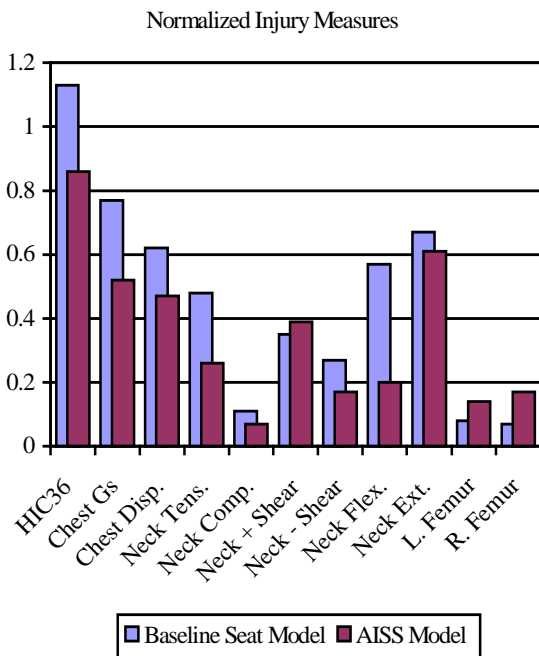


Figure 2: Frontal impact analytical simulation results.

The analytical simulations predicted that almost all of the 50th percentile male injury measures were below the ICPLs for both the AISS and the baseline integrated seat in a simulated 56 kmph rigid barrier crash. The

results further showed that the AISS would improve most occupant injury measures for the 50th percentile male dummy over a baseline integrated seat. The greatest improvements in the AISS simulation were the chest acceleration results which decreased 32%, and chest deflection and HIC results which both decreased 24%. These improvements were primarily attributed to the pretensioner and force limiting features of the seat belt.

Table 1. FMVSS No. 208 NPRM Injury Criteria Performance Limits (ICPLs)	Mid-Sized Male
Head Criteria: HIC (36 ms)	1,000
Neck Criteria: Peak Tension (N) Peak Compression (N) Fore-and-Aft Shear (N) Flexion Bending Moment (Nm) Extension Bending Moment (Nm)	3,300 4,000 3,100 190 57
Thoracic Criteria 1. Chest Acceleration (G) 2. Chest Deflection (mm)	60 63
Lower Ext. Criteria: Femur Load (N)	10,008

AISS Prototypes: Four AISS prototypes were fabricated for testing in the research program. Two seats were evaluated in frontal impact sled tests and two were evaluated in rear impact sled tests.



Figure 3: AISS prototype (front and side view).

Quasar Industries conducted the soft tooling and was the part source for all structural metal for the AISS prototypes. Breed Technologies, Inc. provided the off-the-shelf retractors, pretensioners, and side air bag parts. Johnson Controls Inc. assembled the seat structure and also fabricated and assembled the foam and trim. The photos in Figure 3 are of one of the final prototypes.

Sled Testing: The frontal impact sled test setup is shown in Figure 4. An instrumented 50th percentile male Hybrid III dummy was seated on the AISS and restrained by the integrated seat belt system. As in the analytical modeling, the sled test simulated a 56 kmph full frontal rigid barrier vehicle crash. The peak deceleration was approximately 34.5 G and the pulse duration was 85 msec. The crash pulse is illustrated in Figure 5. A production driver side air bag was fired at 20 msec into the simulated crash event.

For comparison, a baseline seat was also tested under the same sled test conditions. The baseline seat was an integrated seat with a single recliner and adjustable head restraint.

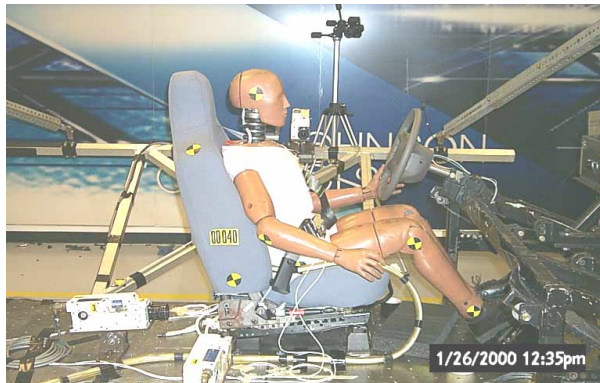


Figure 4: Frontal impact sled test set-up.

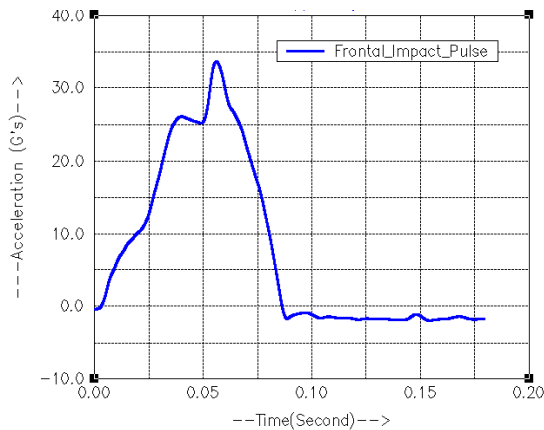


Figure 5: Frontal impact sled test pulse.

Two sled tests were conducted in the frontal impact mode with two of the AISS prototypes (each tested once). In the first AISS sled test, the pretensioner did not function as intended. A metal tab designed to constrain rotation of the unit was bent and slipped away from the slot in the casing. An attempt was made to correct this in the second test. Therefore the normalized injury measures from the second AISS sled test were compared against the results from the baseline seat sled test in the present analysis (Figure 6). As in the frontal impact analytical simulations, most of the

50th percentile male dummy injury measures from the AISS sled test were lower than those from the baseline sled test. Additionally, all of the injury measures were below the ICPLs for the AISS sled test.

Unlike the analytical simulations, the head accelerations were relatively comparable between the baseline seat and the AISS. The peak head acceleration in the baseline seat was 79 Gs and in the AISS it was 80 Gs. The HIC results were also relatively similar; the baseline seat has a HIC result of 923 and the AISS had a HIC result of 911.

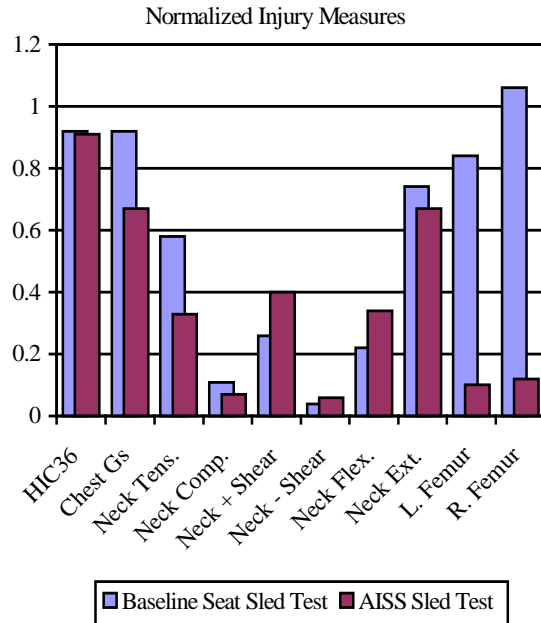


Figure 6: Normalized results from the frontal impact sled tests.

The AISS sled test demonstrated large improvements in peak chest acceleration responses when compared to the baseline seat. (This was also predicted by the analytical simulations.) The dummy in the baseline seat sled test had a chest acceleration result of 55 Gs; whereas the dummy in the AISS sled test had a chest acceleration result of only 40 Gs. This was an improvement of approximately 26%. In the AISS sled test, the load limiter was effective in keeping the chest acceleration levels relatively constant (approximately 40 Gs for 20 msec.). The addition of the pretensioner in the AISS was also able to begin restraining the chest earlier in the event. However post-test inspection of the hardware indicated that the pretensioner had a slight internal malfunction and pulled in only 40 mm of the intended 80 mm of belt. (Thus, further chest acceleration improvements may be expected with full-functionality of the pretensioner.)

Axial neck forces and neck extension moments were also slightly lower in the AISS sled test; whereas neck shear and neck flexion moments resulted in a

slight increase. However, all neck injury measures were well below the ICPLs. This is consistent with other frontal impact testing using the 50th percentile male dummy [12]. Low femur loads resulted in the AISS sled test and were potentially due to anti-submarining effects of the buckle pretensioner. Femur loads in the baseline sled test may have been artificially high due to contact with the steel knee bolster support bracket.

Correlation of the Analytical Simulations to the Sled Test Results: The trends and the timing from the frontal impact analytical simulation results were generally well correlated to the sled test results. For example, comparisons of the chest acceleration traces are found in Figure 7 for the baseline seat and Figure 8 for the AISS.

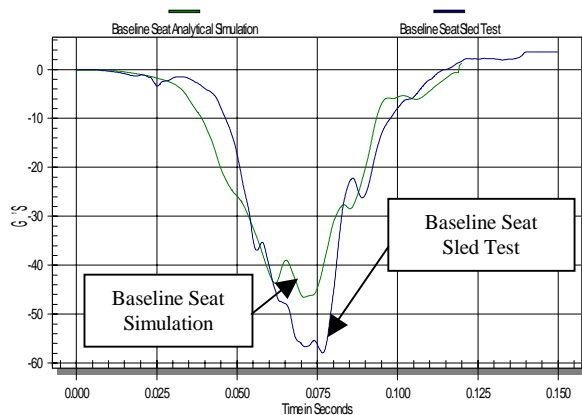


Figure 7: Chest acceleration comparison between the baseline seat sled test and the baseline analytical simulation.

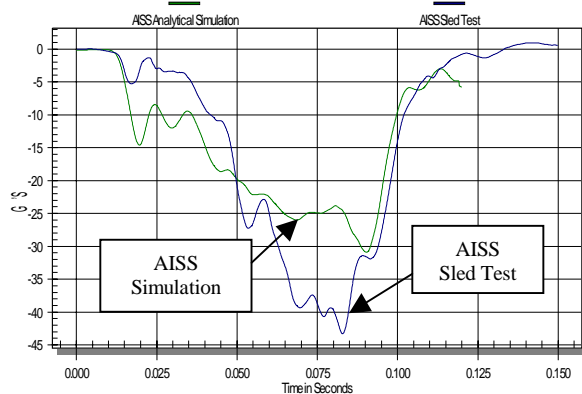


Figure 8: Chest acceleration comparison between the AISS sled test and the AISS analytical simulation.

A few notable differences between the sled test and the simulations resulted in the differences in the peak values. As previously mentioned, the pretensioner in the AISS sled test did not function to its full potential. This is illustrated by the small initial chest acceleration peak in the AISS sled test at 20 msec (Figure 8). However, in the analytical simulation of the AISS, the pretensioner had pulled in the full 80 mm of belt, and

the restraining forces were applied to the dummy's chest at a much higher level (during the same 20 msec time frame in Figure 8). Therefore, this resulted in lower overall peak chest acceleration for the AISS analytical simulation.

The mid portion of the chest acceleration signal for the AISS sled test also exhibited less force limiting effects than the AISS simulation (Figure 8). The AISS sled test maintained a chest acceleration level of 40 Gs for approximately 20 msec; whereas in the AISS simulation, the chest acceleration was maintained at a lower level of 25 Gs for approximately 30 msec. This may be attributed to the physical properties of the mechanical load limiter device. As the belt load increased, the load limiter deformed a mechanical part to maintain a 4 kN load level on the belt, and in the physical device, there was a limited length that the loads could be maintained. However the AISS simulation did not have this limitation and spooled out additional belt material, as necessary.

Other variability between the analytical simulations and the sled tests may have been attributed to assumptions about the material properties and differences in the modeling set-up. This is further discussed in the AISS Modification 2 Final Report [10].

Rear Impact Testing And Simulation

Rear impact crashes account for approximately 5% of motor vehicle fatalities, but account for approximately 30% of motor vehicle injuries [7]. Neck injuries with risk of permanent disability are frequent in low severity rear impact collisions. Because these crashes are common, they can cause human suffering and high societal costs, despite the fact that the injuries are usually classified as "minor"[7]. In higher speed impacts, seats may deform significantly, allowing occupant ramping and potential contact with rear seat occupants. Therefore the AISS project sought to improve rear impact protection by enhancing the seat structure characteristics to minimize both frequent low speed impact injuries, and potentially more severe, but less frequent, high speed impact injuries.

AISS Features for Rear Impact: The AISS design has the following countermeasures for improved occupant crash protection in rear impacts: an integrated seat belt system, dual linear recliners, energy absorbers, and an extended head restraint system. In the AISS design, the integrated seat belt system helped reduce seat back ramping and potential contact with rear seat occupants. The dual linear recliner resulted in uniform loading of the seat back and provided torsional resistance from seat back twist. The energy absorbers also minimized occupant rebound and ramping by adding structural elements that deform plastically in a

controlled manner. The mechanical energy absorbing elements were added in series to both recliners on either side of the seat. Finally, the AISS extended head restraint was fixed in position (i.e., not adjustable). This eliminated the possibility of the head restraint not being positioned correctly for the reduction of whiplash injuries in rear impacts.

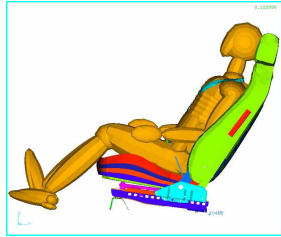


Figure 9: Rear impact simulation of the AISS.

Analytical Modeling: The AISS model (discussed in the frontal section) was also used for conducting rear impact simulations and for designing rear impact countermeasures. As previously mentioned, the seat back frame, the dual linear recliners, and the energy absorbers were optimized for frontal and rearward loading. For rear impacts, the seat back was designed not to yield at 1800 Nm about the h-point [9].

Models of the AISS recliners and energy absorbers are shown in Figure 10. The AISS recliners are bracketed to the seat back frame and are also secured to the seat track supporting plate by a bolt that passes through both the recliner rod end piece and the supporting plate. The energy absorber is positioned underneath the recliner rods and is constructed of two concentric bracket shells. When loaded by the recliner rods, the energy absorbers are designed to deform plastically in a controlled manner (i.e., as the recliner is forced downwards the metal in the energy absorber plates gets rolled inward).

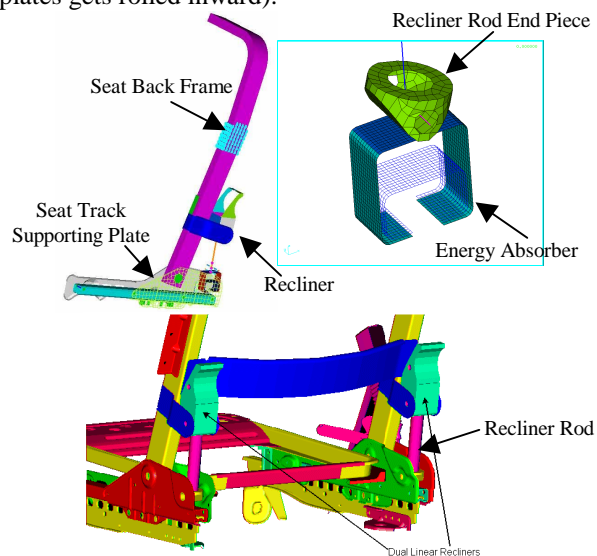


Figure 10: Analytical modeling of the dual linear recliners and rear impact energy absorbers.

The energy absorber was designed to withstand occupant loads to the seat back during normal use, but was designed to yield (a maximum of 30 degrees) when the seat back begins to fail in a rear impact crash [9]. The packaging of the energy absorber bracket in the seat track of the AISS was verified by Johnson Controls, Inc.

Finally, the complete AISS analytical model was coupled with the MADYMO Hybrid III 50th percentile male dummy model and was subjected to a simulated rear impact crash pulse (approximately 18 G peak, 90 msec pulse duration). A baseline integrated seat model (without the energy absorber and dual linear recliner) was also developed and subjected to the identical rear impact simulation for comparison.

Results of the Analytical Simulations: The AISS rear impact simulation results were compared to those from the baseline seat. Figure 11 compares the normalized injury measures. The analytical simulation predicted that all the 50th percentile male dummy injury measures were well below the ICPLs for both the AISS and the baseline integrated seat. The results further showed that the AISS would improve most occupant injury measures for the 50th percentile male dummy in a rear impact crash over a baseline integrated seat. However, the simulations only predicted marginal improvements.

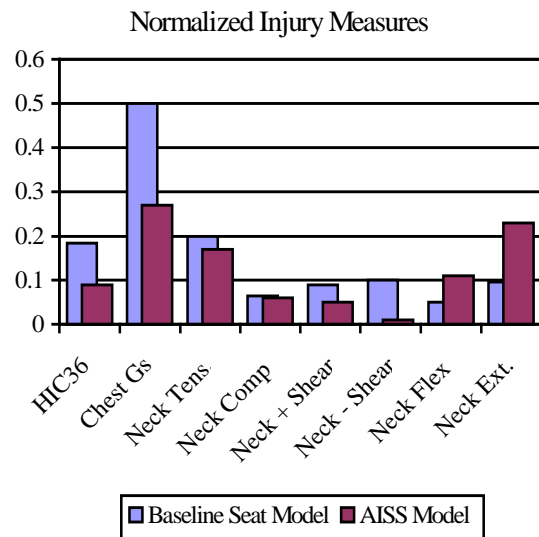


Figure 11: Rear impact analytical simulation results.

Sled Testing: Two of the AISS prototypes were used in rear impact sled tests. The sled test setup is shown in Figure 12. An instrumented Hybrid III dummy was seated on the AISS prototype and restrained by the integrated belt system. The sled test simulated a rear impact pulse with a 18 G peak, 90 msec duration. The sled pulse is illustrated in Figure

13. A baseline seat was also tested under the same sled conditions as the AISS for comparison. The baseline seat was an integrated seat with a single recliner and an adjustable head restraint. The structural energy absorbing elements were also not included.

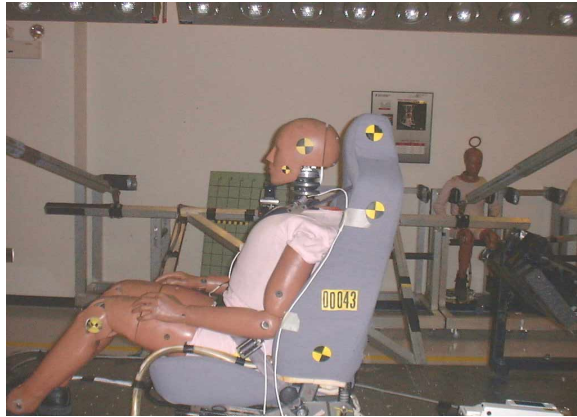


Figure 12: Rear impact sled test set-up.

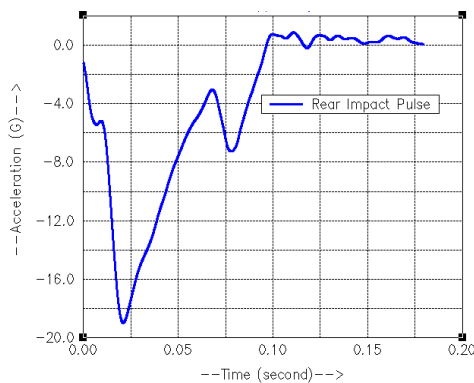


Figure 13: Rear impact sled test pulse.

The normalized injury measures from the second¹ AISS rear impact sled test are plotted in Figure 14, and they are compared to the sled test results using the baseline seat. As in the rear impact analytical simulation, most of the 50th percentile male dummy injury measures from the AISS sled test were lower than those from the baseline seat sled test. Additionally, all of the injury measures were below the ICPLs.

The dummy neck tension and neck extension results were greatly reduced in the AISS sled test. Peak neck tension in the AISS sled test was 38% lower than in the baseline seat sled test. Similarly the dummy's peak upper neck extension moment in the AISS sled test was 29% lower than the baseline seat sled test. It is believed that the extended head restraint and the energy

¹ The second AISS test had improved dummy positioning and was used for comparison.

absorbing elements contributed to the lower neck injury measures.

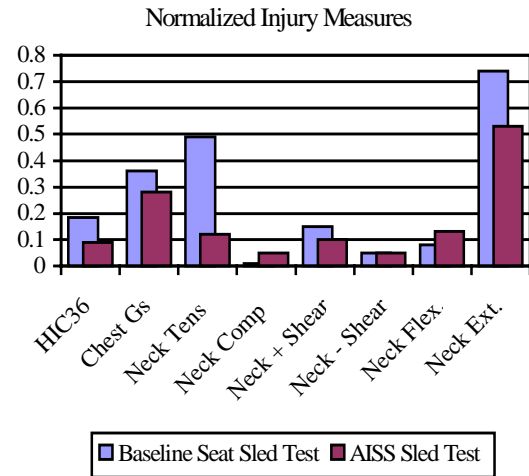


Figure 14: Normalized results from the rear impact sled tests.

The head and chest responses were slightly lower in the AISS rear impact sled test. Initially the dummy started sinking into the seat back until it reached full penetration (at approximately 50 msec). The energy absorber then started to crush and allowed the seat back to yield in a controlled manner (from approximately 60 msec to the end of seat back rotation). This resulted in a reduction of the dummy head and chest accelerations. However, the baseline seat, without the energy absorbing elements, resulted in higher injury measures in the rear impact sled tests. The peak head acceleration in the baseline seat sled test was 39 Gs and the HIC was 184. In the AISS sled test, the peak head acceleration was 31 Gs and the HIC was 90. Chest acceleration results were also reduced from 21 Gs in the baseline sled test to 16 Gs in the AISS sled test.

Correlation of the Analytical Simulations to the Sled Test Results:

The general trends between the AISS and the baseline seat rear impact sled tests were relatively consistent with the model predictions. The head and chest injury reductions predicted in the simulations were evident in the sled tests. However, the reductions in neck extension and neck tension that resulted in the AISS sled test were not predicted by the simulation. The neck tension from the baseline seat sled test and the neck extension from both the baseline seat and AISS sled tests were under-predicted by the simulation. However, in both the two sled tests and in the analytical models, the neck responses independently demonstrated good repeatability. Therefore, there may be some biofidelic shortcomings in how the neck was modeled.

Good correlation resulted in the analytical simulation of the AISS energy absorbing elements.

Figure 15 illustrates the comparison of the analytical model results with the actual post-test hardware from the AISS rear impact sled test.

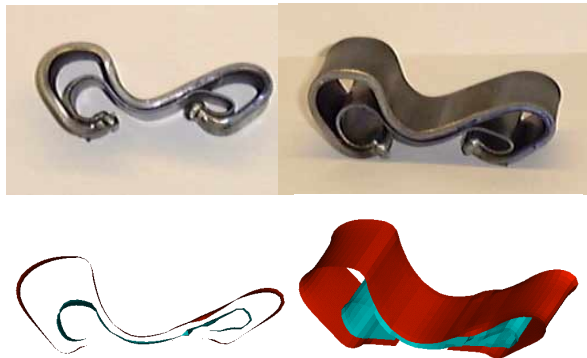


Figure 15: Comparison of analytical modeling of the energy absorbing elements vs. the post-test hardware from the rear impact sled test.

Side Impact Simulation

Side impact crashes of light vehicles, (i.e. passenger cars, light trucks and vans), result in approximately 9,800 fatalities and over 1,020,000 injuries each year. This corresponds to about 30% of vehicles involved in tow away crashes [13]. Therefore, considerable work has been done in the development of effective side impact countermeasures. Some have been incorporated into the vehicle structure while others have been mounted on the seat. The AISS project focused on evaluating the potential of those that could be mounted on the seat itself.

Side Impact Countermeasures: Two side impact countermeasures proposed for the AISS design were independently evaluated through analytical simulations. The countermeasures included: an Inflatable Tubular Cushion (ITC), and a combination head/thorax side impact air bag system.

The ITC system is a seat-mounted tubular bladder that is designed to reduce lateral loads on the occupant and prevent occupant ejection during a side impact collision (Figure 17). The ITC is an inflated tube which is anchored on the outboard side of the seat at two end points (toward the front of the seat pan and the top of the seat back). When deployed, the ITC expands and shortens at the same time. Due to the unique properties of the structural materials and the anchored end points, tension is introduced into the system as the bag inflates. The advantage of the ITC is that it eliminates the need for a reaction surface and consequentially creates a self-supporting inflated unit.

The combination head/thorax side impact air bag system is mounted on the outboard side of the seat frame (Figure 18). The seat trim has a special seam at

the air bag location that splits open from the inflation pressure and allows the air bag to deploy into the vehicle interior. The combination head/thorax side impact air bag has two inflation chambers separated by a vented partition wall. The head/thorax side impact air bag system is designed to protect the occupant by filling the airspace between the intruding door and the occupant as early as possible in the crash event. Upon activation, the thorax chamber is filled directly by the inflator within the first 20 msec. The head chamber is subsequently filled as gas is passed through the vent holes in the chamber partition wall.

Analytical Modeling Description: In the evaluation of the side impact countermeasures, coupled LS-DYNA3D/MADYMO simulations were conducted using the U.S. FMVSS No. 214 side impact crash mode configuration (Figure 16). The AISS model (previously discussed) was incorporated into a full vehicle finite element model of a 1991 Ford Taurus [14]. The MADYMO Side Impact Dummy (SID) model was seated in the AISS model and positioned in the driver location of the full vehicle model. The vehicle was assumed to be stationary in the setup. A moving deformable barrier was modeled and given an initial velocity of 53.4 kmph, crabbed at an angle of 27 degrees. Simulations were conducted to compare the occupant protection provided to the SID in the following three configurations: the AISS with no side impact countermeasure, the AISS with an integrated ITC system, and the AISS with an integrated combination head/thorax side impact air bag system.

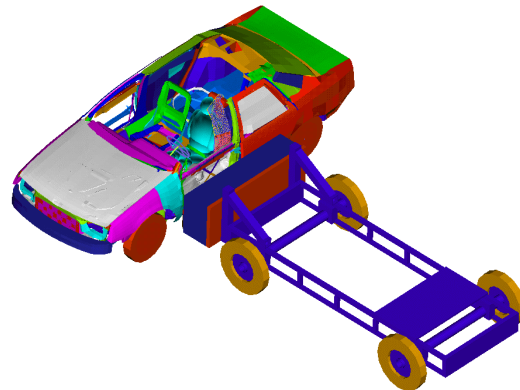


Figure 16: Side impact simulation set-up.

In modeling the two side impact countermeasures for this study, a *representative* model was developed for each system. Neither represented an exact model of a specific system. The primary goals were to have a model of the ITC with approximately the correct inflated size and shape, and a realistic system tension and internal pressure at the time of contact with the occupant. Using this approach, it was not necessary to

model the exact details of the woven ITC material, the inflator properties, the packaging or the inflation process. Instead, the ITC was modeled as an initially flat tube with two end straps for connecting the ITC to the seat structure (Figure 17). Simula Technologies provided a “generic” ITC model and system data to approximate the inflated geometry and internal pressure [9].

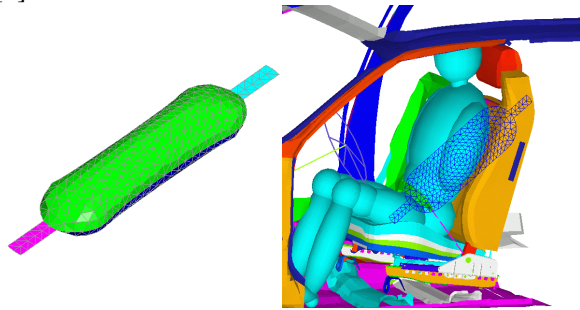


Figure 17: Inflatable Tubular Cushion (ITC) side impact countermeasure and simulation set-up.

Similarly, the goal in modeling the combination head/thorax side impact air bag system was to develop a *representative* model in the side impact simulation (Figure 18). Breed Technologies provided a “generic” combination head/thorax side impact air bag model [10].

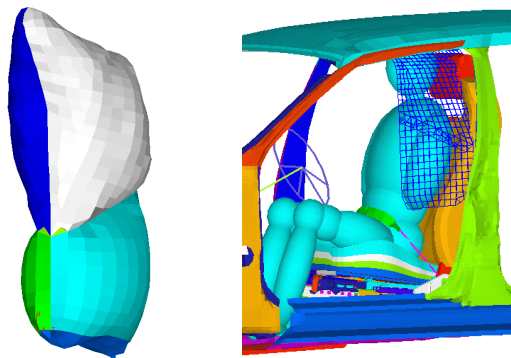


Figure 18: Combination head/thorax side impact air bag system countermeasure and simulation set-up.

Results of the Analytical Simulations: The side impact simulation results of the AISS with the ITC and the AISS with the combination head/thorax side impact air bag system were compared against the results of the AISS simulation without additional side impact countermeasures. Table 2 summarizes the occupant injury results from each simulation.

First, the combination head/thorax side impact air bag model provided improved occupant protection to the SID (over the AISS simulation without additional side impact countermeasures). The top rib Thoracic Trauma Index (TTI) was reduced from 61.1 Gs to 47.6 Gs, and the bottom rib TTI was reduced from 60.2 Gs to 51.3 Gs. The combination head/thorax side impact air bag model filled the air-space between the intruding door and the SID very quickly. This resulted in early restraint being applied to the SID ribs (around 15 msec with the combination head/thorax side impact air bag vs. 28 msec without the air bag). This early restraining force, combined with the energy absorption of the thorax chamber (as gas was vented into the head chamber) resulted in lower peak rib accelerations.

Conversely, the side impact simulation using the AISS and ITC system model resulted in increasing the peak rib accelerations of the SID. Unlike the combination head/thorax side impact air bag, the ITC model was not vented and became very stiff under tension. Even though the ITC model quickly filled the air-space between the intruding door and the SID, the ITC model acted like a rigid spacer, transferring load directly from the door to the SID.

Neither the AISS with the combination head/thorax side impact air bag model nor the AISS with the ITC model predicted improved occupant protection for the pelvis region. Since the combination head/thorax side impact air bag model did not provide coverage of the pelvic region, it had little effect on the pelvic response. However, the AISS with the ITC model actually increased the peak pelvis acceleration. This was attributed to the fact that the ITC model was stiffer in the deployed state and interacted, to some extent, with

	Top Rib		Bottom Rib		Pelvis		T12	
	TTI (G's)	Δ TTI (%)	TTI (G's)	Δ TTI (%)	Peak Acc. (G's)	Δ Peak (%)	Peak Acc. (G's)	Δ Peak (%)
AISS	61.1		60.2		113.6		66.5	
AISS + ITC	66.0	+8.0	73.5	+22.1	127.0	+11.8	77.0	+15.8
AISS +Combination Head/Thorax Bag	47.6	-22.1	51.3	-14.8	110.8	-2.4	64.5	-3.0

the pelvis and left femur of the SID. This resulted in higher levels of pelvic acceleration when trapped between the dummy and the intruding door structure. A similar trend resulted in the T12 response of the SID in the AISS with ITC model; whereas the combination head/thorax side impact air bag model resulted in an earlier interaction and reduced peaks in the T12 acceleration. Therefore, of the two countermeasure models, the AISS with the combination head/thorax side impact air bag predicted improved occupant protection for the SID.

Rollover Simulation

According to the 1999 Fatality Analysis Reporting System (FARS), 10,142 people were killed as occupants in light vehicle rollovers, including 8,345 killed in single-vehicle rollovers [15]. Using data from the 1995-1999 National Automotive Sampling System (NASS), an estimated 253,000 light vehicles were towed from a rollover crash each year (on average), and 27,000 occupants of these vehicles were seriously injured [15]. Therefore, the data presented above demonstrates that rollover crashes create a serious safety problem to motor vehicle occupants. The AISS project therefore explored potential seat countermeasures that could improve rollover crash protection and also contribute to passenger compartment intrusion resistance.

Rollover Countermeasures: Seat belts are currently the most significant restraint for occupants in rollover crashes because they help prevent occupant ejection from the vehicle. The AISS incorporates a seat integrated belt system which improves occupant belt fit and couples the occupant to the seat. The torso belt was also designed to limit belt system loads to 4 kN (to optimize frontal impact protection) while sustaining loads capable of retaining the occupant within the compartment during rollover crashes. A buckle pretensioner was incorporated in the AISS to take-up slack in the belt system and reduce occupant excursion toward the roof in a rollover event. The AISS was also designed with an 815 mm tall head restraint system to reduce structural intrusion from roof crush. The head restraint design provides a minimal backset between the occupant's head and the head restraint.

Analytical Modeling Description: The AISS analytical model (discussed previously) was incorporated into the driver position of a full vehicle finite element model of a 1991 Ford Taurus [14]. A MADYMO Hybrid III 50th percentile male dummy model was positioned in the AISS. The integrated seat belt was attached to eliminate occupant ejection, and 80 mm of belt was pulled into the retractor to simulate the

pretensioner activation at time=0 (during the initial phase of rollover).

Coupled LS-DYNA3D/MADYMO simulations of a vehicle rollover test were conducted. The particular test set-up involved a vehicle mounted on a rollover cart, which was inclined at an angle of 60 degrees with respect to a horizontal datum, at a height of 1.22 meters. The vehicle was placed on the cart such that the driver's side of the vehicle was closest to the ground. The cart was then accelerated to a velocity of 48 kmph and suddenly decelerated to a 0 kmph stop. The sudden change in the rollover cart velocity sent the vehicle into flight at 48 kmph. The vehicle then rolled in the air and hit the ground with the leading edge of the roof (on the driver's side of the vehicle).

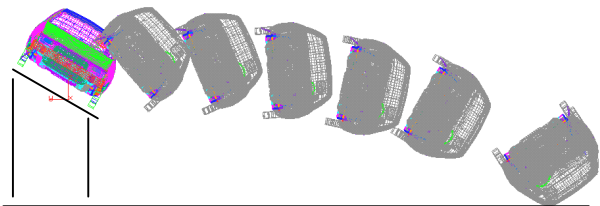


Figure 19: The rigid free-flight phase of the rollover simulation.

The analytical simulation of the rollover test was carried out in two phases. The first was a rigid free-flight phase (Figure 19) and second was a deformable vehicle-to-ground impact phase (Figure 20).

The first phase of simulation began with the free-flight of the vehicle into the air where no ground contact or deformation to the vehicle occurred. To take advantage of this fact, the entire vehicle was considered rigid to improve the required simulation time. Once the vehicle hit the ground, at the end of this phase, the velocities were recorded for use in the second phase.

The vehicle contacted the ground plane with a 48 kmph velocity in the y-direction and a 20.5 kmph velocity in the z-direction at approximately 580 msec into the simulation. The vehicle model also rotated approximately 105 degrees about the x-axis from the initial position on the cart. These final velocities and rotation from the rigid phase were used as initial conditions for the second (deformable) phase.

The second phase of the simulation started when the vehicle hit the ground (Figure 20). In this phase, the yaw and pitch of the vehicle were not considered, as they were not significant compared to the roll of the vehicle, and a constant rotation of 180 degrees/sec was assumed. The vehicle model was deformable in this phase, and the occupant was free to move (as opposed to the first phase in which the occupant was restrained in position). The contact friction between the ground and the vehicle was assumed to be 0.3.

The rollover simulations were performed with two different head restraint positions of the AISS. The top surface of the head restraint at highest position was

flush with the top of the crown of a seated 95% percentile male occupant head. The lower head restraint was positioned such that the top of the head restraint was flush with top of the head of a seated 50% percentile male occupant.

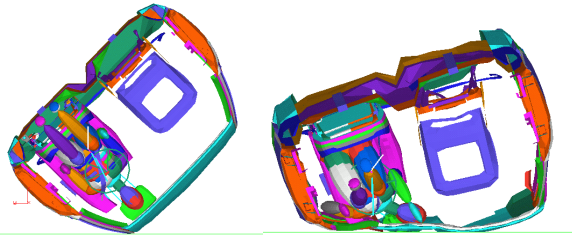


Figure 20: The deformable phase of the rollover simulation.

Results of the Analytical Simulations: Two head restraint positions were evaluated in the analytical rollover simulation, as discussed above. In the extended head restraint simulation, the resultant head acceleration was reduced approximately 14 percent from the lower head restraint position. Similarly, upper neck lateral shear forces and neck extension loads were also reduced 38 percent and 32 percent, respectively. However, only small reductions in upper neck fore/aft shear and axial loading resulted in the extended head restraint position.

While the extended head restraint prevented larger intrusion into the occupant compartment during roof crush, it only yielded marginal improvements in occupant protection over the lower head restraint position. This resulted for a number of reasons. The rollover test simulated in the model was particularly demanding on the structural integrity of the roof. Since the model was not fully-validated in the rollover crash mode, significant structural deformation of the vehicle roof resulted (Figure 20). The inner structural details of the model can affect occupant injury, as they determine the specific hit location of the occupant inside the compartment. Also, there was not a significant difference between the height of the extended head restraint and the lower head restraint position (27 mm). Therefore, only marginal gains in reducing the injury parameters resulted. Future work could involve improving the vehicle finite element model validation in the rollover crash mode and conducting additional simulations to better demonstrate the AISS benefits of the integrated belt system, the pretensioner activation, and the extended head restraint system.

CONCLUSION

An Advanced Integrated Safety Seat (AISS) was evaluated in the front, rear, side, and rollover crash modes using coupled LS-DYNA3D/MADYMO analytical simulations. Frontal and rear impact crash modes were also experimentally evaluated using sled

tests with AISS prototypes. Comparative tests with a baseline integrated seat were also conducted.

In the frontal crash mode, the AISS pretensioner and 4 kN force limiter contributed to reducing the chest injury measures on the Hybrid III dummy. This was reflected in both the analytical simulations and the prototype sled test results. The analytical model also demonstrated relatively good trend correlation with the experimental sled testing.

In the rear impact mode, the dual linear recliner, energy absorber, and extended head restraint system also helped to reduce head, neck, and chest injury numbers on the Hybrid III dummy. The analytical model was also able to predict the energy absorber bracket deformation that resulted in the sled test.

A full vehicle finite element model of the 1991 Ford Taurus was used in the side impact simulations of the FMVSS No. 214 crash test configuration. Analytical models of a “generic” Inflatable Tubular Cushion and a combination head/thorax side impact air bag were each incorporated into the AISS model for comparison. The combination head/thorax side impact air bag model predicted improved occupant protection for the SID, overall, when placed between the intruding door structure and the occupant. The early restraining force, combined with the energy absorption of the thorax chamber (as gas was vented into the head chamber) resulted in lower injury measures. Future AISS improvements could be made in protecting the pelvis of the SID dummy in side impact crashes.

Rollover simulations were also conducted with a full vehicle finite element model of the 1991 Ford Taurus. The simulations predicted that the AISS extended head restraint prevented larger intrusion into the occupant compartment during roof crush and reduced occupant injury. However, future work in refining the full vehicle finite element model in the rollover crash mode could better demonstrate the rollover benefits of the AISS integrated belt system, buckle pretensioner, and extended head restraint system.

ACKNOWLEDGMENTS

The authors wish to thank Simula Technologies for the Inflatable Tubular Cushion data, and Breed Technologies for the head-thorax combination side impact air bag data.

REFERENCES

- [1] National Highway Traffic Safety Administration, *Traffic Safety Facts 1999: A Compilation of Motor Vehicle Crash Data from the Fatality Analysis Reporting System and the General Estimates System*, DOT HS 809 100, December 2000, www.nhtsa.dot.gov.

- [2] Gupta, V., Menon, R., Gupta, S., Mani, A., Shanmugavelu, I., *Advanced Integrated Structural Seat Final Report*, February 1997, Docket No. NHTSA-1998-4064.
- [3] Cole, J.H., *Developing a Cost Effective Integrated Structural Seat*, SAE Paper No. 930109, Society of Automotive Engineers, Warrendale, PA, 1993.
- [4] Interim Final Rule for FMVSS No. 208, National Highway Traffic Safety Administration, Federal Register, Volume 65, No. 93, page 30680, May 12, 2000, NHTSA Docket No. NHTSA-2000-7013.
- [5] *Effectiveness of Occupant Protection Systems and Their Use*, U.S. Department of Transportation, National Highway Traffic Safety Administration, National Center for Statistics and Analysis, May, 1999.
- [6] Hollowell, W.T., Gabler, H.C., Stucki, S.L., Summers, S., Hackney, J.R., *Updated Review of Potential Test Procedures for FMVSS No. 208*, October 1999, NHTSA Docket No. NHTSA-2000-7013.
- [7] Gupta, V., Menon, R., Gupta, S., Mani, A., Shanmugavelu, I., Kossar, J., *Improved Occupant Protection through Advanced Seat Design*, Proceedings from the Experimental Safety Vehicle Conference, Melbourne, Australia, 1996, Paper 96-S1-O-08.
- [8] Kallieris, D., Rizzetti, A., Mattern, R., Morgan, R., Eppinger, R., Keenan, L., *On the Synergism of the Driver Air Bag and the 3-Point Belt in Frontal Collisions*, 39th Stapp Car Crash Conference Proceedings, Society of Automotive Engineers, Warrendale, PA, 1995.
- [9] Rashidy, M., Gunasekar, T.J., Gupta, S., Griffioen, J., and Howard, J., *Advanced Integrated Safety Seat, DTNH22-97-C-07003, Task Order #01, Final Report*, July 1999.
- [10] Rashidy, M., Gunasekar, T.J., Morris, R., Munson, B., and Lindberg, J.A., *Advanced Integrated Safety Seat, DTNH22-97-C-07003, Task Order #01, Modification 2, Final Report*, August 2000.
- [11] Notice of Proposed Rulemaking for FMVSS No. 208, National Highway Traffic Safety Administration, Federal Register, Volume 63, No. 181, September 18, 1998, page 49987, NHTSA Docket No. NHTSA-1998-4405.
- [12] NHTSA Docket Number NHTSA-2000-7013-16. www.dms.gov, June 20, 2000.
- [13] Samaha, R.R., *B.02.02.03 Upgrade Side Crash Protection*, NHTSA Research & Development Project Summaries, www.nhtsa.dot.gov, June 1998.
- [14] Varadappa, S., Shyo, S., Mani, A., *Development of a Passenger Vehicle Finite Element Model*, DOT HS 808 145, Contract DTNH22-92-D-07323, November 1993.
- [15] Notice of Final Decision for Consumer Information Regulations on Rollover Resistance, National Highway Traffic Safety Administration, Federal Register, Volume 66, No. 9, January 12, 2001, page 3388.
- [16] Bardini, R., and Hiller, M., *Contribution of Occupant and Vehicle Dynamics Simulation to Testing Occupant Safety in Passenger Cars During Rollover*. SAE 1999-01-0431, Society of Automotive Engineers, Warrendale, PA, 1999.
- [17] Chace, M.A., and Wielenga, T.J. *A test and Simulation Process to Improve Rollover Resistance*, SAE 1999-01-0125, Society of Automotive Engineers, Warrendale, PA, 1999.
- [18] Gupta, V., Gunasekar, T.J., Rao, A., Kamarajan, J., *Reverse Engineering method for developing full vehicle finite element models*, SAE 1999-01-0083, Society of Automotive Engineers, Warrendale, PA, 1999.